CrossMark

ORIGINAL ARTICLE

# Strength and Bearing Capacity of Ring Footings Resting on Fibre-Reinforced Sand

Vaibhav sharma[1] · Arvind kumar[2]

**Abstract** Stress–strain response of fibre-reinforced and unreinforced sands has been studied by using large direct shear and drained triaxial shear tests. Influence of fibre content (0.50, 0.75, 1.00, and 1.25%), normal stress (for direct shear) and confining pressure (for triaxial shear test), relative density of the unreinforced and fibre-reinforced sand (medium i.e. 50%, and dense i.e. 70%) has been studied. Moreover shear strength parameters obtained from direct shear and triaxial shear tests have been used to calculate the Ultimate bearing capacity (UBC) of ring footings by proposing an empirical expression. UBC calculated theoretically, by using the shear strength parameters obtained from direct shear and triaxial shear test, has been compared with the experimental UBC. Fibres inclusion in the sand not only increases the shear strength of sand-fibre matrix but significantly improves the stress–strain response. Shear strength parameters obtained from direct shear tests have been found to be lesser than that of the triaxial shear test. UBC calculated, using shear strength parameters, from triaxial shear test gave more conservative values than that of the direct shear test.

✉ Vaibhav sharma
civil.vaibhav.sharma@gmail.com

Arvind kumar
agnihotriak@nitj.ac.in

1 Department of Civil Engineering, Dr. B R Ambedkar National Institute of Technology, Jalandhar, Punjab 144011, India

2 Dr. B R Ambedkar National Institute of Technology, Jalandhar 144011, India

## Introduction

A foundation engineer generally comes across a problem of designing foundations for various structures such as buildings, bridges, dams, towers and water tanks etc. Ring footings are more suitable for axi-symmetric structures like towers, chimneys, etc.in comparison to circular footings. An expression to calculate ultimate bearing capacity of ring footing has been the major concern for geotechnical engineer. Few researchers have contributed in this area and tried to arrive at an expression, analytically as well as experimentally. An expression for calculating the settlement and reactive pressure of a rigid smooth ring foundation subjected to central vertical load was given by Egorov [1]. An expression was developed to determine the settlement and tilt of ring footings resting on a linearly deformable layer of finite thickness. For simplifying the calculations, non-dimensional charts and tables were presented by Egorov et al. [2]. Saha [3] conducted model tests on ring footings resting on the surface of sand and subjected to central vertical load. An empirical equation was developed to calculate the ultimate bearing capacity of ring footing based on intersection tangent method. Haroon and Misra [4] carried out an experimental investigation on annular footings resting on sand subjected to central vertical load. From test results an empirical equation was developed to calculate the ultimate bearing capacity and shape factors. The behavior of rigid ring footings, resting on sand, subjected to central vertical load was studied. Based on non-dimensional analysis, an empirical equation to calculate the ultimate bearing capacity of ring footing has been developed by Kakroo [5]. Many researchers have carried out the experimental and analytical studies on ring footings for its better understanding. Al-Sanad [6] and Ismael [7] carried out field plate load tests on ring footings resting on

🍦 Springer

dense calcareous sand. Many investigators [[8–17]] carried out experimental and numerical studies on ring footings. Naseri and Hosseininia [18] carried out numerical computations using finite difference method in order to investigate the elastic settlement of ring foundations resting over an elastic half space. Results are presented in the form of graphs and the corresponding mathematical expressions are proposed for the influence factors. An approximate solution for the calculation of bearing capacity of ring footing has been presented by many researchers, but still there is a need to develop an expression for bearing capacity calculation which can be used by practicing engineers with confidence.

Researchers across the world are improving the geotechnical properties of weak soil by reinforcing it with planar (geotextiles, geogrids, etc.), 3D (geocells, etc.), and random inclusions of discrete elements (fibres, etc.). One of the major benefits of random inclusions in the soil over other type of reinforcement is the absence of weak zone in soil strata. Gray and Ohashi [19] carried out direct shear tests on dry sand reinforced with natural and synthetic fibres plus metal wires. Results indicated that with the inclusion of randomly distributed fibres in soil, there is increase in peak shear strength and post peak reduction in shear strength is limited. Gray and Al-Refeai [20] carried out triaxial shear compression tests to compare the stress–strain response of sand reinforced with fabric layers, and randomly distributed fibre inclusions. Both types of reinforcements improved strength, axial strain at failure and reduced post peak loss in strength. At very low strains (<1%), fabric inclusions resulted in decrease in compressive stiffness as compared to fibre inclusions. Freitag [21] studied the unconfined compressive strength of plain and fibre reinforced sandy clay, when compacted as different water content. Results indicated that randomly distributed fibres in a fine grained soil cause greater strength and toughness. Michalowski and Zhao [22] derived a failure criterion by using energy-based homogenization scheme for fibre-reinforced granular soil. Laboratory triaxial shear tests were also carried out to check its agreement with the model prediction. Michalowski and Cermak [23] conducted triaxial shear compression tests on fibre-reinforced sand. Moreover, a theoretical model was developed to check its agreement with the experimental work. Consoli et al. [24] studied the load settlement response from plate load tests on circular footing resting on fibre-reinforced soil. Test results showed that stress–strain response changes dramatically with fibre inclusions in the soil. Consoli et al. [25] conducted model plate load tests on circular footing resting on layers of soil improved by using cement and fibres. Maximum improvement was observed, when cement and fibres both were introduced into soil, in terms of shear strength. Babu and Vasudevan [26] presented the strength and stiffness behavior of soil reinforced with coir fiber. Results indicated that inclusion of coir fibers in the soil increases deviator stress upto 3.5 times that of the plain soil. Yetimoglu et al. [27] carried out california bearing ratio (CBR) tests to investigate the load penetration behavior of sand when reinforced with randomly distributed fibre reinforced sand layer overlying soft clay. There is an appreciable increase in peak piston load when fibres are included in the sand. Diambra et al. [28] carried out triaxial shear compression and extension tests. Fibres contribution was remarkable in compression than in extension. Theoretical model was developed to validate the experimental results. Sadek et al. [29] carried out extensive direct shear tests to, (1) supplement the data available in the literature on the behavior of fibre-reinforced sands; (2) study the effect of several parameters which are known to affect the shear strength of fibre-reinforced sands; and (3) investigate the effectiveness of current models in predicting the improvement in shear strength of fibre-reinforced sand. Result indicates the existence of a fibre-grain scale effect which is not catered for in current prediction models. Li and Zornberg [30] conducted triaxial shear and fibre pullout tests on specimens to evaluate how fibre tension is mobilized for varying shear strain levels. A revision to an existing design methodology was proposed in which the individual contribution of fibres and soil matrix is quantified based on the strain levels. Kumar and Gupta [31] conducted unconfined compressive strength (UCS) tests and split tensile strength (STS) tests to evaluate the strength properties of clay when mixed with rice husk ash, pond ash, cement, and fibres. Results indicated that addition of fibres causes increase in UCS, STS, and axial strain at failure.

In this paper, large direct shear and triaxial shear tests were carried out in order to arrive at the shear strength parameters. Moreover, the stress–strain response of sand was studied when mixed with different percentages of fibres and at different relative densities. From the calculated shear strength parameters ultimate bearing capacity (UBC) of model footings was calculated by modifying the expression given by Kakroo [5], using results of both the direct shear and triaxial shear tests. Furthermore, UBC calculated theoretically was compared with the UBC obtained from model plate load tests conducted on model footings.

## Experimental Program

Shear strength parameters have been calculated using large direct shear and triaxial shear tests.
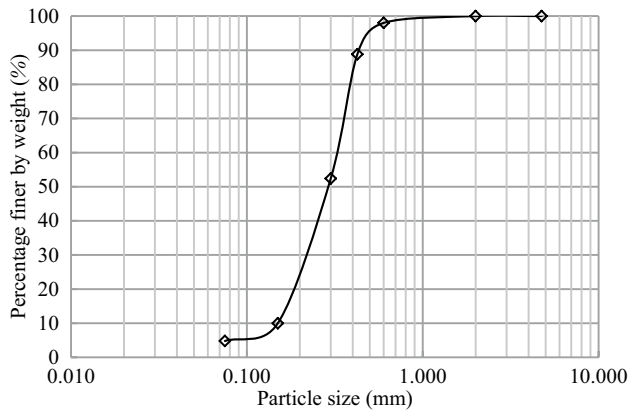
**Fig. 1** Particle-size distribution of sand

## Materials Used and Testing Procedure

### Soil Used

Fine grained sand, classified as poorly graded (SP) according to unified soil classification system, was used in the testing program. Specific gravity ($G_s$) of sand was found to be 2.65. Maximum, and, minimum dry unit weights were found to be 16.8 and 13.9 kN/m$^3$, respectively. The particle size distribution was determined by dry sieving method, and the particle size distribution curve is shown in Fig. 1. The effective size ($D_{10}$) and mean size ($D_{50}$) of the sand was 0.150 and 0.290 mm respectively. The coefficient of curvature ($C_c$) and coefficient of uniformity ($C_u$) for the sand was 0.97 and 2.21 respectively.

### Fibres Used

Macro-synthetic and non-corrosive ENDURO HPP 45 fibres were used as reinforcement in the sand. The physical and chemical properties of fibres as supplied by the manufacturer are shown in Table 1.

### Tests Performed

Large direct shear and consolidated drained (CD) triaxial shear tests were conducted on sand reinforced with different fibre content (0.50, 0.75, 1.00, and 1.25%), by dry weight of the sand-fibre composite, at respective relative densities (RD). Tests were conducted at two RD's i.e., 50% RD (medium) and 70% RD (dense). For the calculation of shear strength parameters of unreinforced and randomly distributed fibre reinforced sand, two types of tests were carried out. Large box direct shear tests were conducted as per [32] and drained (CD) triaxial shear tests were conducted as per [33].

### Model Testing

Total 65 model plate load tests were carried out as shown in Table 2. A testing-cum-loading frame assembly was used for conducting model tests. The soil bed was prepared in a testing tank with inside dimensions of 1.5 m long, 1.5 m wide and 1 m deep. The model footings were made from mild steel, and were corrected to the desired size, thickness (25 mm) and shape (ring and circular). One circular footing and four ring footings were used in this study. Diameter for circular footing was 0.3 m and, the ratio of inner

**Table 1** Chemical and physical properties of fibres

| | | | |
|---|---|---|---|
| Fibre length | 45 mm | Acid and salt resistance | High |
| Type | Macro | Ignition point | >550$^o$c (1022 °F) |
| Absorption | Nil | Melt point | 164$^o$c (328 °F) |
| Specific gravity ($G_f$) | 0.91 | Thermal conductivity | Low |
| Electrical conductivity | Low | Alkali resistance | Alkali proof |
| Tensile strength (N/mm$^2$) | 400 | Elastic modulus (N/mm$^2$) | 7000 |
| Diameter (mm) | 0.95 | Shape | Continuously deformed |

**Table 2** Test plan for model tests

| Series | Type of sand | Type of footing (ri/ro) | Fibre content (%) | (h1/B)* | Number of tests |
|---|---|---|---|---|---|
| A | Unreinforced | 0, 0.3, 0.4, 0.5, and 0.6 | 0 | 0 | 5 |
| B | Reinforced | 0, 0.3, 0.4, 0.5 and 0.6 | 0.5, 0.75, 1.00 and 1.25 | 0.50, 0.75 and 1.00 | 60 |
| Total tests | | | | | 65 |

B is the diameter of circular footing and outer diameter for ring footing

*Thickness of fibre reinforced sand layer

radius to outer radius of ring footings, ($r_i/r_o$) 0.3, 0.4, 0.5, and 0.6, were used in the study by keeping the outer diameter of ring to be constant i.e. 0.3 m. The model footing was loaded until the failure of sand (large uniform settlement corresponding to very small increment in load) or the manually operated hydraulic jack gets fully extended. Two 0.01 mm sensitivity dial gauges were placed on either and opposite side of the footing to calculate settlement for every equal increment of load.

For ring footings, it was not possible to place hydraulic jack directly on them because it may slip through the opening of the ring footings. So, to avoid this, first a loading platform was placed on ring footing followed by the hydraulic jack. Then loading of ring footing was possible. Test setup is shown in Fig. 2a. Detail of loading platform is shown in Fig. 2b, c.

*Preparation of Bed and Test Procedure*

Test bed consisting of two layers of sand was prepared. First, bottom unreinforced sand layer was filled, by using sand raining technique, at a known and desired density followed by leveling after reaching desired height. Relative density of unreinforced sand obtained from sand raining technique was 50% for all the model tests. Secondly, RDFS layer was filled on the top. For laying top RDFS layer, first

dry weights of fibres and sand were calculated, using equations (1) and (2). This means that fibres were added as a replacement of sand.

$$W_{RDFS} = V \times \gamma_{RDFS} \tag{1}$$

$$W_{RDFS} = W_s + W_f = p_s W_{RDFS} + p_f W_{RDFS} \tag{2}$$

where, $W_{RDFS}$ is dry weight of RDFS layer. $W_s$ is the dry weight of sand and $W_f$ is dry weight of fibres. $\gamma_{RDFS}$ is dry unit weight of RDFS layer; $V$ is the total volume of RDFS layer to be placed; $p_s$ and $p_f$ are the percentages of sand and fibres in RDFS layer, respectively.

For the preparation of RDFS layer, sand and fibres were hand mixed. The RDFS layer was filled in equal shifts of 100 mm and compacted. Tank's inner walls were marked so as to ensure the proper thickness of layers. Random mixing, of fibres, is difficult to achieve because there are chances of segregation. It is due to the different specific gravities of both, fibres and sand. So, to minimize this problem, dry fibres (calculated as explained before) were soaked in water before adding to sand for mixing. This was done in order to make them wet, which in turn coats fibre with thin layer of water. Then they were transferred to sieves so that the excess water gets removed and then transferred to the sand for mixing. Each layer of RDFS was compacted using a wooden rammer so that the layer achieves desired
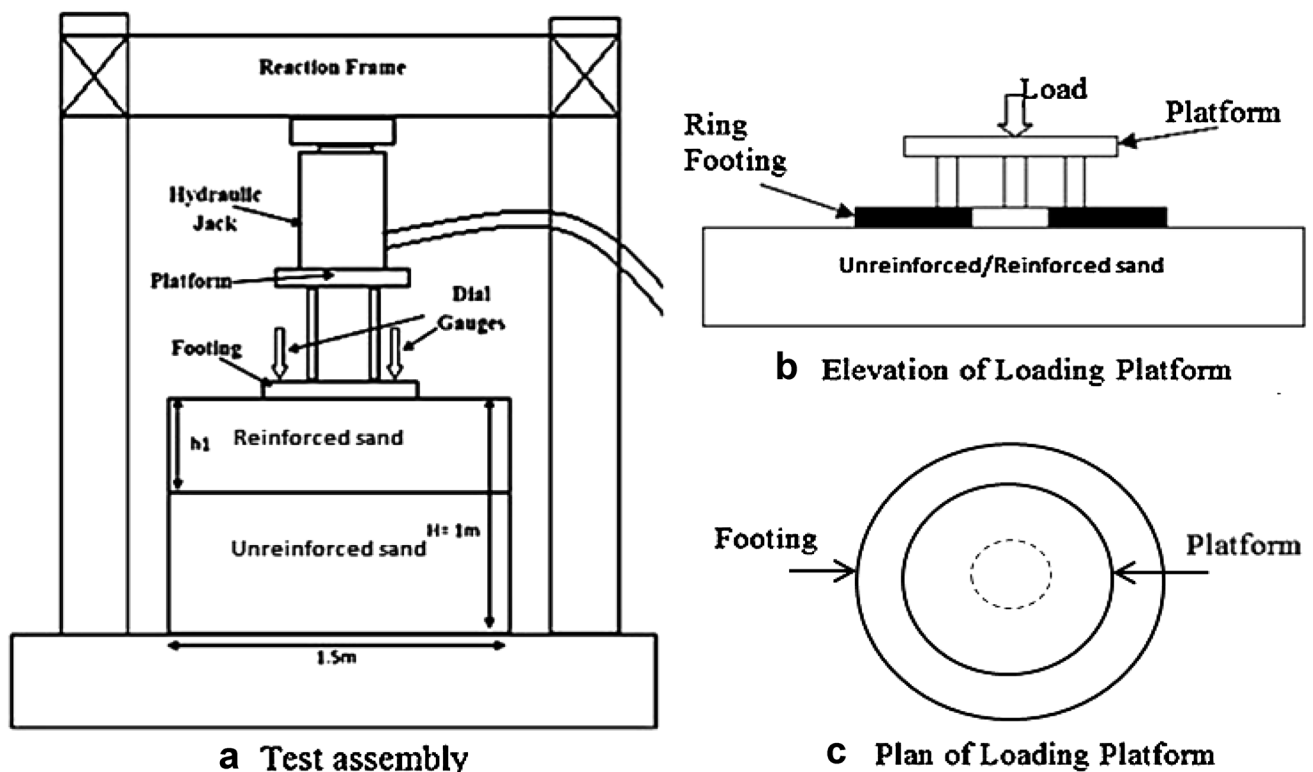


**Fig. 2** Test setup, **a** test assembly, **b** elevation of loading platform and **c** plan of loading platform

thickness. After filling of RDFS layer, it was leveled carefully. Footing was centered carefully, so that the loading should be concentric. Then loading platform was placed over the footing (in case of ring footing) centered followed by the placing of hydraulic jack over it as shown in Fig. 2a. Two sensitive dial gauges were placed on either and opposite side of the footing to measure the settlement. Then equal load increment was applied through manually operated hydraulic jack.

## Theoretical Calculation of UBC of Ring Footings

Kakroo [5] studied the behavior of rigid ring footings subjected to central vertical load resting on sand. Tests were conducted on model footings having external diameters of 100, 200 and 300 mm, with radius ratio of 0.0, 0.2, 0.3, 0.4, 0.6 and 0.8, embedded at depth ratio of 0, 1/3 and 2/3 on dry sand at relative densities of 20, 55, and 75%. The effects of the aforementioned variables on the load-settlement, bearing capacity, contact pressure distribution and rupture surface for rigid ring footings were investigated. Based on the non-dimensional analysis, the following empirical equation was developed and is shown in Eq. (3).

$$q_u = \gamma R D_r \tan\phi\left(236 + 465n - 1420n^2 + 745n^3 + 282\frac{D_f}{R}\right) \tag{3}$$

where $q_u$ is the ultimate bearing capacity of footing used. $\gamma$ is the unit weight of soil used. $R$ is the external radius of footing. $\phi$ is the angle of internal friction of soil used. $n$ is the radius ratio ($r_i/r_o$). $D_r$ is the relative density of soil and $D_f$ is the embedment depth of footing.

Equation (3) was modified on the basis of the experimental tests conducted on ring footings by introducing soil cohesion term same as that given by Terzaghi [34]. The experimental tests were conducted on surface ring

and circular footings resting on randomly distributed fibre-reinforced sand overlying unreinforced sand. The details of the tests conducted are presented elsewhere [35]. Four ring footings with $r_i/r_o = 0.3$, 0.4, 0.5, and 0.6 were used, whereas one circular footing was used. The external radius of both the ring and circular footings was kept constant and only the internal radius of ring footing was varied. Equation (3) given by Kakroo [5] was modified after considering the effect of cohesion as under.

$$q_u = 1.2cN_c + \gamma R D_r \tan\phi\left(236 + 465n - 1420n^2 + 745n^3 + 282\frac{D_f}{R}\right) \tag{4}$$

where, $c$ is the cohesion of soil used, and $N_c$ is the bearing capacity factor given by Terzaghi [34].

## Results and Discussions

Results have been presented and discussed in two parts. In the first part, shear test (direct shear and triaxial shear) results are presented and discussed. In the second part, model test results are presented and discussed.

### Shearing Test Results

Figures 3a, 4 and 5a show the stress–strain curve of fibre-reinforced and unreinforced sand with different RD's, normal stresses, and fibre content, respectively. It can be inferred from Fig. 3a that as the RD of the fibre-reinforced or unreinforced sand is increased from 50 to 70%, there is improvement in peak stress. Moreover, it can be seen that there is decrease in post peak reduction for shear stress (for 50% RD), and there is post peak gain in shear stress (for 70% RD). When RD of the unreinforced sand is increased from 50 to 70%, the peak shear stress is increased from 62.49 to 74 kN/m² respectively. Furthermore, when
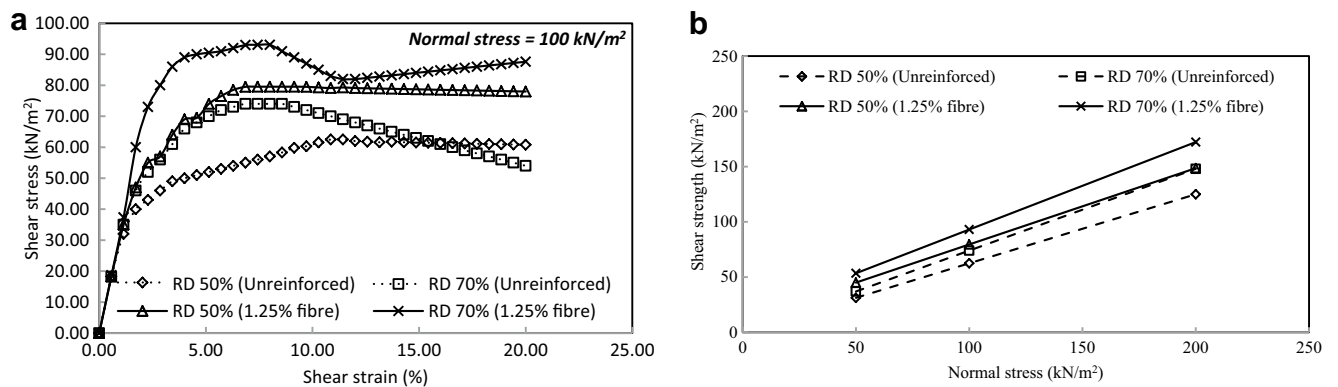


**Fig. 3** **a** Stress–strain response for fibre-reinforced and unreinforced sand at different relative densities, **b** failure envelope of unreinforced and fibre-reinforced sand at different RDs
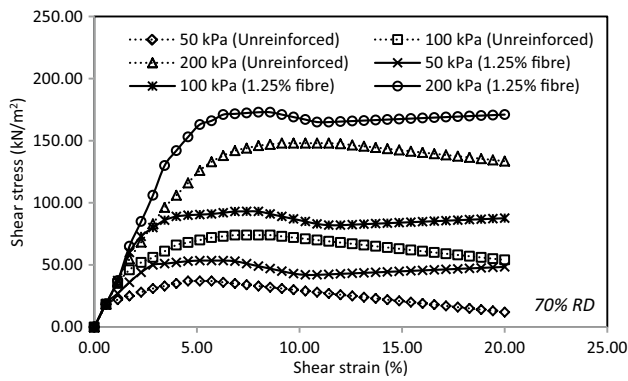
**Fig. 4** Stress–strain response for fibre-reinforced and unreinforced sand at different normal stresses

RD of fibre-reinforced sand is increased from 50 to 70%, the peak shear stress increases from 79.54 to 93.05 kN/m$^2$. Figure 3b shows the failure envelope of unreinforced

and fibre-reinforced sand compacted at different RDs. The angle of internal friction and cohesion has been improved when RD of the sand is increased from 50 to 70%.

Figures 6a, 7, and 8a, shows the stress–strain response of unreinforced and fibre-reinforced sand at different RDs, confining pressures, and, fibre content. It can be inferred from Fig. 6a that as the RD of the fibre-reinforced or unreinforced sand is increased from 50 to 70%, there is improvement in peak deviator stress. Moreover, it can be seen that there is decrease in post peak reduction for deviator stress (for 50% RD), and there is post peak gain in deviator stress (for 70% RD). Similar kind of behavior has taken place in direct shear test. When RD of the unreinforced sand is increased from 50 to 70%, the peak deviator stress is increased from 202.43 to 225.46 kN/m$^2$, respectively. Furthermore, when RD of fibre-reinforced sand is increased from 50 to 70%, the peak deviator stress increases from 294.78 to 337.44 kN/m$^2$. Figure 6b shows the failure envelope of unreinforced and fibre-reinforced sand compacted
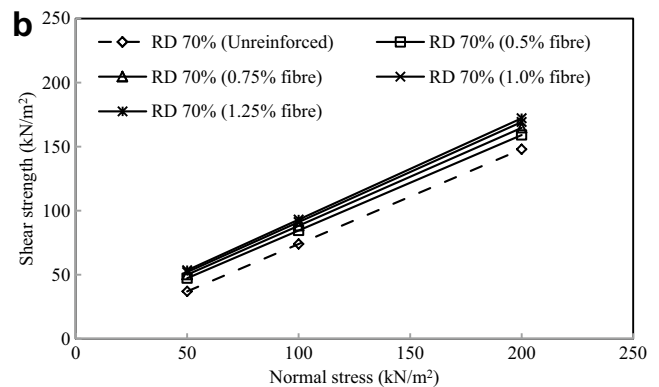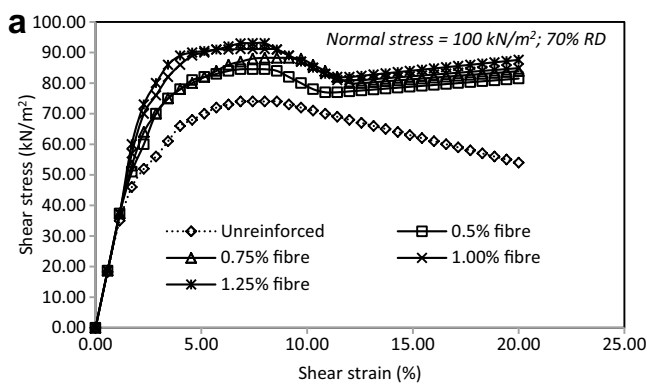


**Fig. 5** **a** Stress–strain response for fibre-reinforced sand at different fiber content. **b** Failure envelope of unreinforced and fibre-reinforced sand at different fiber content
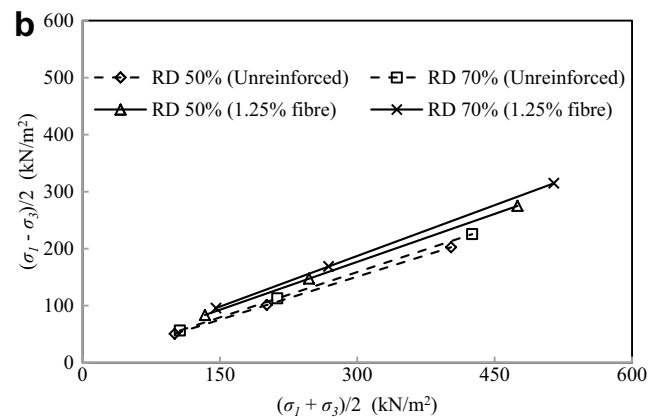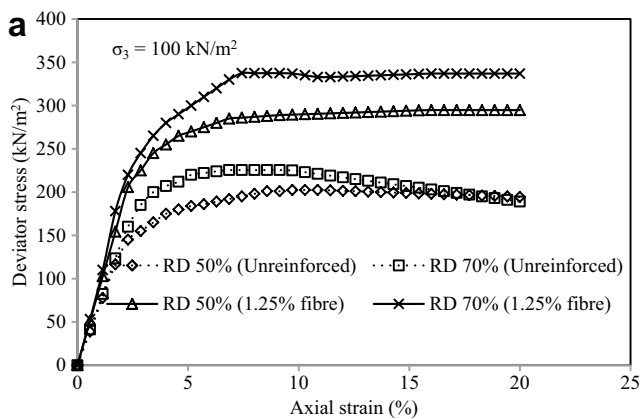


**Fig. 6** **a** Stress–strain response for fibre-reinforced and unreinforced sand at different relative densities. **b** Peak-strength envelope for unreinforced and fibre reinforced sand
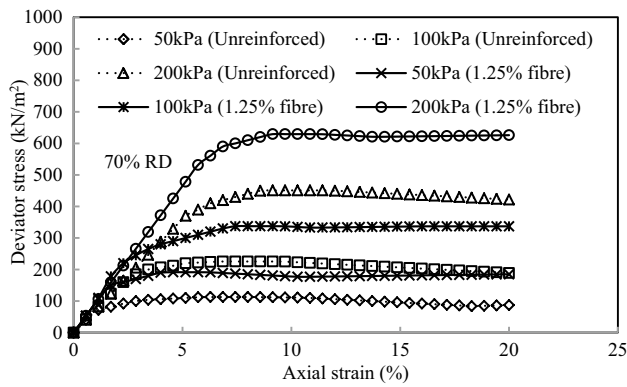
**Fig. 7** Stress–strain response of unreinforced and fibre reinforced sand at different confining pressures

at different RDs. The angle of internal friction and cohesion has been improved when RD of the sand is increased from 50 to 70%. This increase in shear stress is attributing the effect of relative density on the soil-fibre matrix. As the density of the sand-fibre matrix is increased, the amount of sand as well as fibres gets increased by keeping the volume of the matrix constant, which corresponds to the denseness of the sand-fibre matrix. Due to this denseness of the sand-fibre matrix shear stress gets increased.

Figure 4 shows the stress–strain response of unreinforced and fibre reinforced sand at different normal stresses. It can be clearly seen from Fig. 4 that as the normal stress of the same sample of sand is increased, there is significant improvement in peak shear stress. When normal stress on unreinforced sand compacted at 70% RD, is increased from 50 to 100 kN/m², and then to 200 kN/m²; then the peak shear stress is increased from 37 to 74 kN/m² and then to 147.99 kN/m², respectively. Furthermore, When normal stress on fibre-reinforced sand is increased from 50 to 100 kN/m², and then to 200 kN/m²; then the peak shear

stress is increased from 53.47 to 93.05 kN/m² and then to 172.90 kN/m², respectively.

Figure 7 shows the stress–strain response of unreinforced and fibre reinforced sand at different confining stresses. It can be clearly seen from Fig. 4 that as the confining pressure is increased from the same sample of sand, there is significant improvement in peak deviator stress. When confining pressure on unreinforced sand compacted at 70% RD, is increased from 50 to 100 kN/m², and then to 200 kN/m²; then the peak deviator stress is increased from 112.73 to 225.46 kN/m² and then to 450.92 kN/m², respectively. Furthermore, when confining pressure on fibre-reinforced sand is increased from 50 to 100 kN/m², and then to 200 kN/m²; then the peak deviator stress is increased from 191.48 to 337.44 kN/m² and then to 629.34 kN/m², respectively. This increase in shear stress is due to the normal pressure (for direct shear) and confining pressure (for triaxial shear) of the sand-fibre matrix. As and when normal pressure or confining pressure of sand-fibre matrix is increased there is reduction in the lateral displacement of sand-fibre matrix which results in the increase in shear stress.

Figure 5a shows the stress–strain response of fibre-reinforced sand at different content of fibres. It can be inferred from Fig. 5a that as the fibre content is increased from 0.50 to 1.25%, there is increase in peak shear stress. It can also be seen from the Fig. 5a that there is significant change in the behavior of stress–strain response when fibres are introduced in the sand. Post peak shear stress has been found out to be increasing when shear strain is more than 10%. When fibre content is increased from 0.50 to 1.25%, the peak shear stress is increased from 84.54 to 93.05 kN/m², respectively. Fibre inclusion in the sand not only increases the peak shear stress but also improves the overall performance of matrix (sand-fibre) even at larger strains. Figure 5b shows the failure envelope of unreinforced and fibre-reinforced sand at different fibre content. The angle
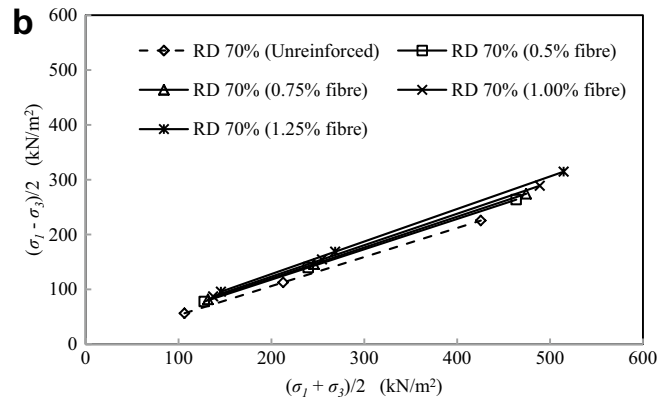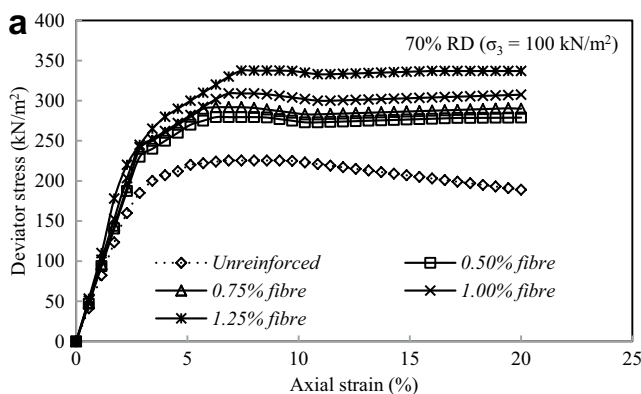


**Fig. 8 a** Stress–strain response of unreinforced and fibre-reinforced sand at different fiber content. **b** Peak-strength envelope for unreinforced and fibre-reinforced sand at different fiber content

of internal friction and cohesion has been improved when fibre content is increased from 0.5 to 1.25%.

Figure 8a shows the stress–strain response of fibre-reinforced sand at different content of fibres. It can be inferred from Fig. 8a that as the fibre content is increased from 0.50 to 1.25%, there is increase in peak deviator stress. It can also be seen from the Fig. 5a that there is significant change in the behavior of stress–strain response when fibres are introduced in the sand. Post peak shear stress has been found out to be increasing when shear strain is more than 10%. When fibre content is increased from 0.50 to 1.25%, the peak deviator stress is increased from 279.52 to 337.44 kN/m$^2$, respectively. Fibre inclusion in the sand not only increases the peak shear stress but also improves the overall performance of matrix (sand-fibre) even at larger strains. Figure 8b shows the failure envelope of unreinforced and fibre-reinforced sand at different fibre content. The angle of internal friction and cohesion has been improved when fibre content is increased from 0.5 to 1.25%. The angle of internal friction and cohesion of unreinforced and fibre-reinforced sand has been presented in Table 3. This increase in shear stress is due to the contribution of sand- fibre interaction. As the sand-fibre interaction helps in gaining shear stress due to fibre-sand friction. Hence, on increasing the percentage of fibre, available surface area of fibre for frictional force (between fibre and sand) to be mobilized will be more, which results in stress increases in the sand-fibre matrix.

Table 3 shows the shear strength parameters obtained from both the direct shear and triaxial shear tests. It also shows the comparison of the present study with the study reported in literature [29]. Sadek et al. [29] carried out direct shear tests on fibre reinforced fine and coarse sand

compacted at 55% relative density. The fibres used were nylon fishing wire fibres with aspect ratio of 40. Fibres used in the present study are macro-synthetic with aspect ratio of 47. Comparison shows that there is good agreement between the present study and the one reported in literature. It can be clearly seen from the Table 3 that direct shear test results gave higher values of the shear strength parameters than that from triaxial shear test. Figure 9 shows the variation of principal stress at failure versus fibre content at different RDs. It can be inferred from Fig. 9 that as the fibres are added in the sand there is improvement in the principal shear stress at failure. Moreover, with the increase in fibre content; principal stress at failure is increased. Furthermore, increasing the confining pressure increases the principal stress at failure.
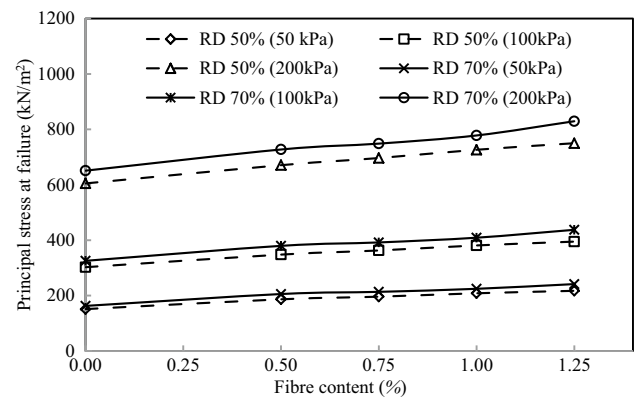


**Fig. 9** Variation of principal shear stress versus fibre content at different RDs

**Table 3** Shear strength parameters

| RD (%) | Fibre content (%) | Direct shear test (present study) | | Triaxial shear test (present study) | | Sadek et al. [29]* | |
|---|---|---|---|---|---|---|---|
| | | | | | | Ottawa sand (fine sand) | Black green line sand (coarse sand) |
| | | Cohesion (kN/m$^2$) | $\phi$ (°) | Cohesion (kN/m$^2$) | $\phi$ (°) | $\phi$ (°) | $\phi$ (°) |
| 50 | 0.00 | 0.00 | 32.00 | 0.00 | 30.20 | – | – |
| | 0.50 | 8.70 | 32.80 | 7.00 | 31.80 | 31.6 | 37.8 |
| | 0.75 | 9.50 | 33.60 | 8.00 | 32.60 | – | 37.9 |
| | 1.00 | 10.00 | 34.00 | 9.60 | 33.43 | 32.9 | 39.5 |
| | 1.25 | 10.50 | 34.62 | 10.50 | 31.10 | – | – |
| 70 | 0.00 | 0.00 | 36.50 | 0.00 | 32.00 | – | – |
| | 0.50 | 10.00 | 36.70 | 8.50 | 33.60 | – | – |
| | 0.75 | 11.80 | 37.40 | 9.30 | 34.20 | – | – |
| | 1.00 | 13.00 | 38.00 | 10.40 | 35.00 | – | – |
| | 1.25 | 13.90 | 38.36 | 11.50 | 36.40 | – | – |

*Direct shear tests were conducted at 55% relative density

## Model Tests

The improvement in performance of RDFS layer overlying unreinforced sand layer was studied by using a non-dimensional factors as:

Improvement in terms of ultimate bearing capacity [BCR: bearing capacity ratio (36)], which compares the bearing capacity of circular footing resting on unreinforced sand to that of bearing capacity of given footing resting on RDFS overlying sand. It is defined in Eq. (5).

$$BCR = \frac{\textit{Ultimate bearing capacity of given footing resting over RDFS layer overlying unreinforced sand}}{\textit{Ultimate bearing capacity of circular footing resting over unreinforced sand}} \qquad (5)$$

In this paper, UBC was obtained by using tangent intersection method. In this method initial linear portion of pressure settlement curve is extended and final linear portion is extended backward, so that both extended lines intersect at a point. Pressure corresponding to this intersection point is taken as ultimate bearing capacity. Effect of internal diameter of rings, percentage of fibres and thickness of fibre reinforced soil layer has been studied using the improvement factor previously explained in Eq. (5).

### Effect of Internal Diameter of Ring Footings

Figure 10 shows the pressure settlement curve of different types of footings when thickness of RDFS layer is 0.75B with 1% fibre content in it. It can be inferred from Fig. 10 that as the internal diameter of ring footing is increased bearing capacity is first increased up to radius ratio ($r_i/r_o = n$) of 0.4, thereafter it reduces. Sawwaf and Nazir [37] carried ou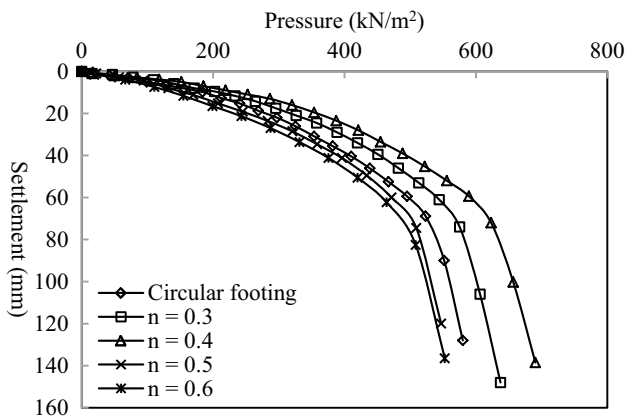t experimental study on ring footings resting on geogrid reinforced sand and found out that for radius ratio of 0.4, optimum behavior of ring footing was observed. This behavior of ring footing is due to the interference effect of ring footing's internal diameter. According to Terzaghi [34], whenever a footing (placed over soil) is loaded three zones gets developed under it. These are zone I (remains in elastic equilibrium and moves with the footing), zone II (radial shear zone, which pushes the zone III), and zone III (rankine's passive zone). As the footing advances in downward direction, zone II pushes the zone III outwards. As this case is similar to the interference effect of closely spaced footings, zone III from both the interfering footings gets intersected, which further causes the arching of the soil in zone III, and helps in improving bearing pressure. This effect is found to be limited up to radius ratio of 0.4; thereafter no arching of soil takes place. It can also be inferred from Fig. 4 that the pressure settlement curve for circular footing is lower than that of ring footing with radius ratio of 0.4. Ultimate bearing capacity for circular footing, and ring footing with radius ratio of 0.4, was observed to be as 505 and 585 kN/m$^2$, respectively.

Figure 11a–c, show the variation of BCR with different types of footings for different percentages of fibres, when $h1/B$ is 0.5, 0.75 and 1, respectively. It can be observed from Fig. 11a–c that as the radius ratio increases up to 0.4, BCR value increases, thereafter it decreases. On increasing radius ratio beyond 0.5 not much significant change in BCR has been observed for all the thicknesses of RDFS layers and percentages of fibres. From Fig. 11a, it can be inferred that when thickness of RDFS layer is 0.5B with 1% fibre content, BCR value for radius ratio of 0 (circular), 0.3, 0.4, 0.5, and 0.6, was observed as 2.44, 2.74, 2.74, 2.39, and 2.33, respectively. From Fig. 11b, it can be inferred that when the thickness of RDFS layer is 0.75B with 1% fibre content, BCR value for radius ratio of 0, 0.3, 0.4, 0.5, and 0.6, was observed as 2.71, 2.93, 3.14, 2.56, and 2.48, respectively. Figure 11c shows that when the thickness of RDFS layer is 1.0B with 1% fibre content, BCR value for radius ratio of 0, 0.3, 0.4, 0.5, and 0.6, was observed as, 2.78, 3.02, 3.26, 2.71, and 2.60, respectively.

### Effect of Fibre Percentage

Figure 12 shows the pressure settlement curve for ring footing with radius ratio of 0.4 with different percentages of fibres and $h1/B = 0.75$. It has been observed from Fig. 12
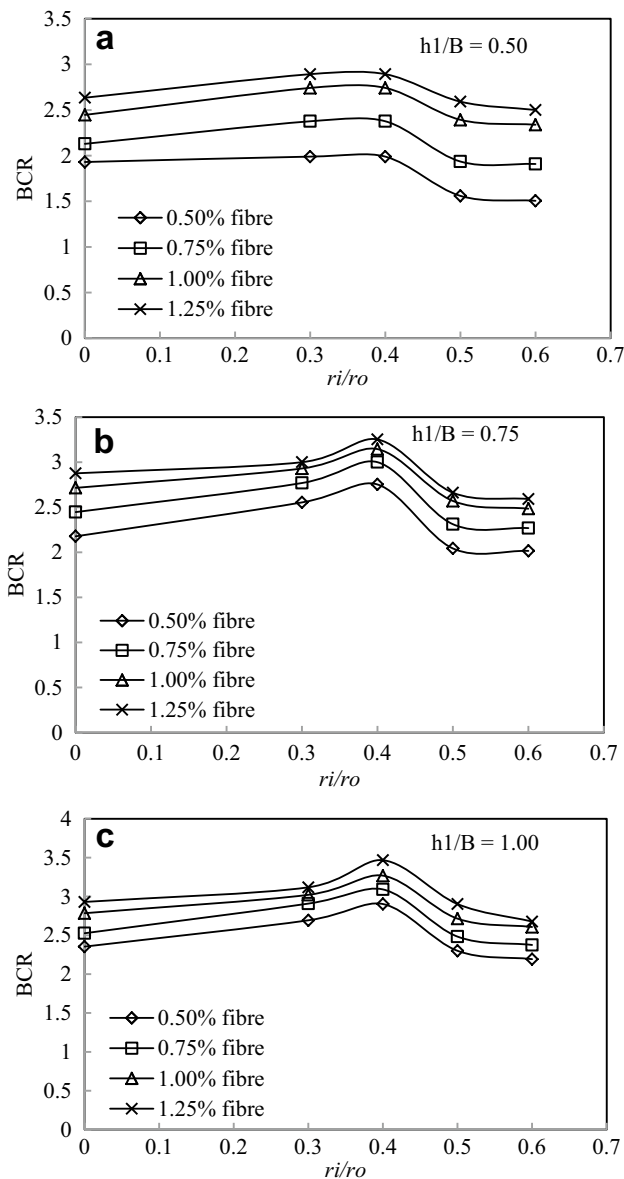
**Fig. 10** Pressure settlement curve of different footings; h1/B = 0.75; and 1% fibre

**Fig. 11** Variation of BCR with $r_i/r_o$; **a** $h1/B = 0.5$; **b** $h1/B = 0.75$; and **c** $h1/B = 1.00$



**Fig. 12** Pressure settlement curve of ring footing with radius ratio of 0.4 and $h1/B = 0.75$

bearing capacity than that of the case when no fibre is there in the matrix. Moreover, when the percentage of fibre goes on increasing; more soil gets replaced by fibres and after a certain critical increase in percentage of fibres, transition of this fibre-soil interaction takes place into fibre–fibre interaction; which reduced the rate of improvement in bearing capacity. From Fig. 12, it can be observed that when percentage of fibre is increased from 0 to 1.25, the ultimate bearing capacity is 211, 512, 558, 585, and 605 kN/m$^2$, respectively.

Figure 13a–c show the variation of BCR with fibre percentage, when h1/B = 0.5, 0.75, and 1, respectively. It has been observed from Fig. 13a–c that as the percentage of fibre is increasing BCR value increases. But beyond a value of 1% fibre; this rate of increment in BCR is reduced, showing that optimum percentage of fibre is 1%. From Fig. 13a, it can be inferred that, for fibre percentage of 0.5, 0.75, 1.0, and 1.25, BCR value is observed as 2.15, 2.72, 2.96, and 3.12, respectively. From Fig. 13b, it can be inferred that, for fibre percentage of 0.5, 0.75, 1.0, and 1.25, BCR value is observed as 2.75, 3.00, 3.15, and 3.25, respectively. From Fig. 13c, it can be inferred that, for fibre percentage of 0.5, 0.75, 1.0, and 1.25, BCR value is observed as 2.90, 3.09, 3.27, and 3.47, respectively.

### Effect of Thickness of RDFS Layer

Figure 14 shows the pressure settlement curve of ring footing with radius ratio of 0.4 with 1% fibre percentage in RDFS layer. It has been observed from Fig. 14 that as the depth of RDFS layer increases from 0 to 1.0B, there is significant improvement in ultimate bearing capacity of footing. Moreover, increasing the thickness of RDFS layer beyond 0.75B, rate of increase in baring capacity is reduced. This is due to the fact that, as the significant depth of isolated circular footing is well known,

that as the percentage of fibres increases from 0.5 to 1.25, there is marked improvement in ultimate bearing capacity. Furthermore, when percentage of fibre is increased from 1 to 1.25, rate of increase in the ultimate bearing capacity decreases which shows that the optimum percentage of fibre is 1. Fibre-soil matrix gains its strength from two types of interaction phenomenon; (a) soil–soil interaction, and (b) fibre-soil interaction. For case (a), when there is no fibre in a soil matrix, only way of gaining strength is due to the interaction between the soil particles themselves. For case (b), when fibres are added in a soil matrix, soil–soil interaction as well as fibre- soil interaction takes place. This fibre-soil interaction further improves the ultimate
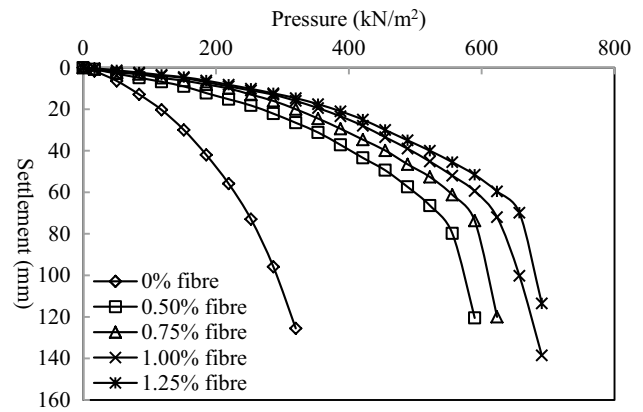
**Fig. 14** Pressure settlement curve for ring footing with radius ratio of 0.4 with 1% fibre in RDFS layer
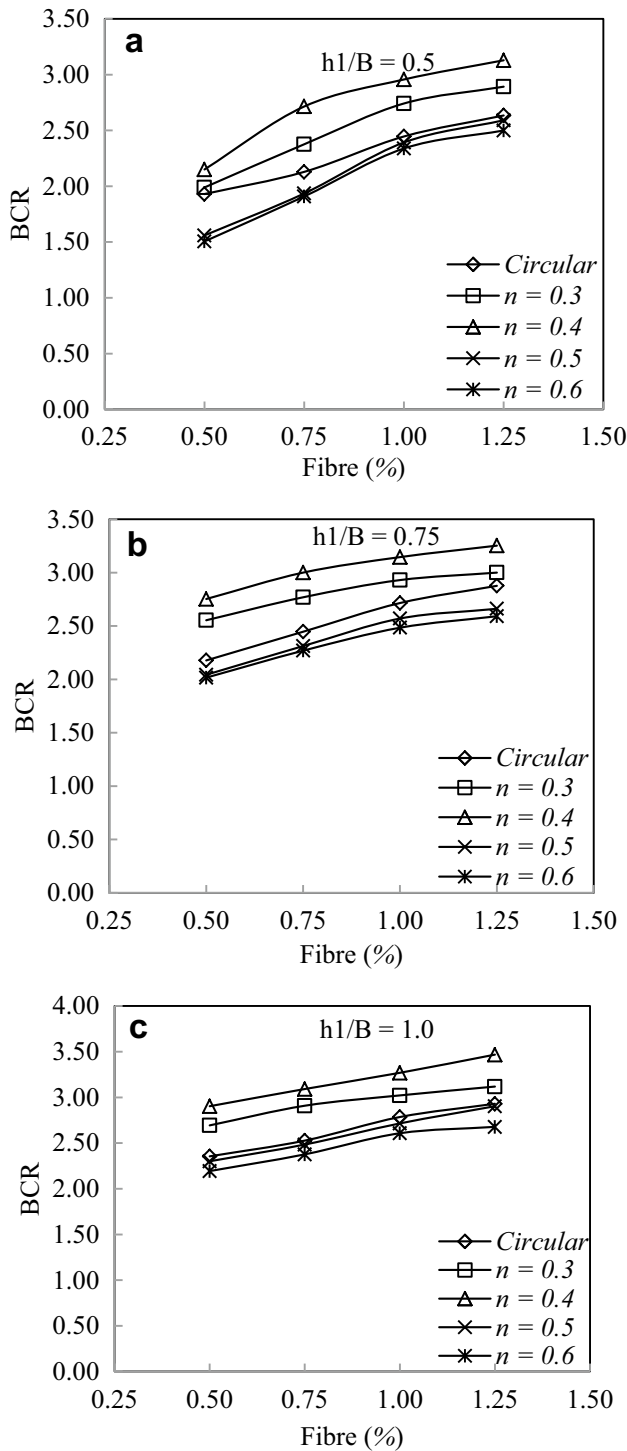
**Fig. 13** Variation of BCR with fiber content; **a** $h1/B = 0.5$; **b** $h1/B = 0.75$; and **c** $h1/B = 1.0$

but for the case of ring footing this significant depth is still not clear. So, it can be said that the optimum value of thickness of RDFS in this case is around 0.75B, and beyond this if, thickness is increased; the ultimate be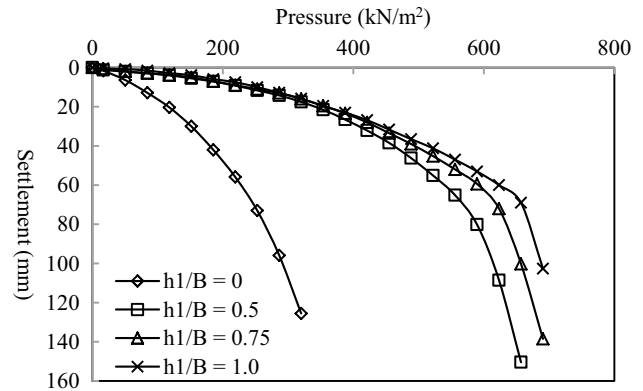aring capacity of ring footing will increase but to a lesser extent, as compared to that of thickness increment from 0.5B to 0.75B. From Fig. 14, it has been observed that for $h1/B = 0$, 0.5, 0.75, and 1.0, the ultimate bearing capacity is 211, 550, 585, and 608 kN/m$^2$, respectively.

Fig. 15a–d show the variation of BCR with $h1/B$ with 0.5, 0.75, 1, and 1.25% fibre in RDFS layer, respectively. It has been observed from Fig. 15 a, b, c and d that as the thickness of RDFS layer is increased, BCR value increases. Furthermore, the increase in BCR value is more significant up to $h1/B = 0.75$, but increasing thickness beyond this value rate of increase in BCR value decreases. From Fig. 15a, it has been observed that as the thickness of RDFS layer is increased from 0.5B to 1.0B with two increments of 0.25B; BCR value for ring footing with radius ratio of 0.4 is observed as 2.15, 2.75, and 2.90, respectively. Similarly from Fig. 15b, BCR value for the same condition is 2.72, 3.00, and 3.09, respectively. Similar behavior is observed in Fig. 15c, d respectively.

## Comparison of Theoretical and Experimental UBC of Ring Footings

Figure 16a, b, shows the comparison of UBC of ring footings calculated theoretically and experimentally, from the results of direct shear tests, and triaxial shear tests, respectively. It can be inferred from both the figures that experimental values of UBC were on higher side than that of the theoretical values. Moreover, UBC calculated using shear strength parameters obtained from direct shear tests gave more correlated values with the experimental values, and the UBC calculated by using triaxial shear test results were found to be on the conservative side. Tables 4 and 5 shows the comparison of UBC calculated by using parameters of direct shear and triaxial shear tests with the experimental.
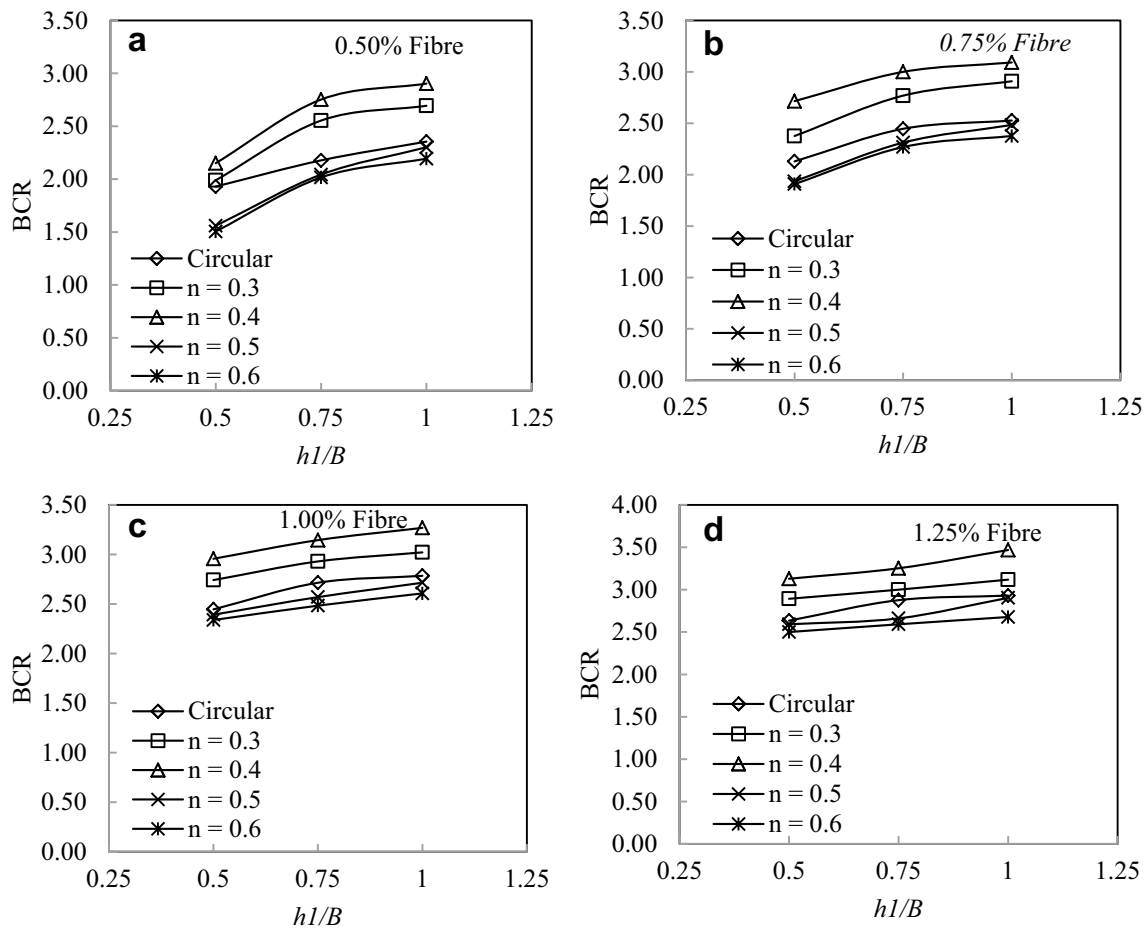
**Fig. 15** Variation of BCR with *h1/B*; **a** 0.5% Fibre; **b** 0.75% Fibre; **c** 1.0% Fibre; and **d** 1.25% Fibre
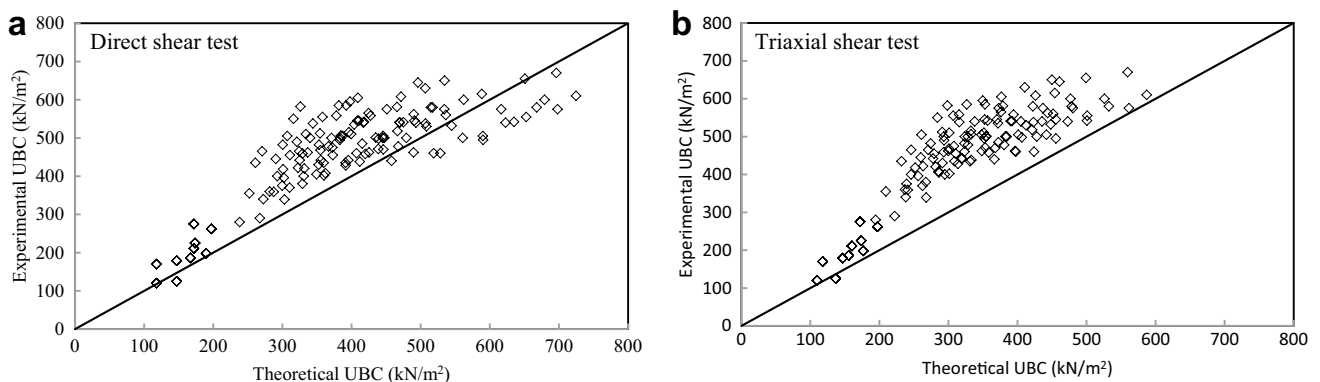


**Fig. 16 a** Comparison of theoretical and experimental UBC of ring footings from direct shear results, **b** comparison of theoretical and experimental UBC of ring footings from triaxial shear test results

## Conclusions

Stress–strain response of fibre-reinforced and unreinforced sand has been studied by using large direct shear and triaxial shear tests. Moreover shear strength parameters obtained from direct shear and triaxial shear tests were used to calculate the UBC of ring footings by modifying the empirical expression given by Kakroo [5]. UBC calculated theoretically both from the shear strength parameters obtained from direct shear and triaxial shear

**Table 4** Comparison of UBC calculated by using parameters of direct shear and triaxial shear tests with the experimental

| *ri/ro* | *h1/B* | Fibre content (%) | RD (%) | UBC (kN/m²) | | |
|---|---|---|---|---|---|---|
| | | | | Direct shear | Triaxial shear | Experimental |
| 0.00 | 0.00 | 0.00 | 50.00 | 167.01 | 155.55 | 186.00 |
| 0.30 | | | | 189.70 | 176.69 | 198.00 |
| 0.40 | | | | 172.00 | 160.21 | 211.00 |
| 0.50 | | | | 147.02 | 136.93 | 125.00 |
| 0.60 | | | | 117.94 | 109.85 | 120.00 |
| 0.00 | 0.50 | 0.50 | | 287.53 | 241.11 | 359.00 |
| | | 0.75 | | 302.06 | 256.18 | 396.00 |
| | | 1.00 | | 310.90 | 279.32 | 455.00 |
| | | 1.25 | | 320.94 | 293.72 | 490.00 |
| 0.30 | | 0.50 | | 310.39 | 262.58 | 370.00 |
| | | 0.75 | | 325.11 | 277.83 | 442.00 |
| | | 1.00 | | 334.04 | 301.16 | 510.00 |
| | | 1.25 | | 344.22 | 315.71 | 538.00 |
| 0.40 | | 0.50 | | 292.56 | 245.83 | 400.00 |
| | | 0.75 | | 307.14 | 260.94 | 505.00 |
| | | 1.00 | | 315.99 | 284.12 | 550.00 |
| | | 1.25 | | 326.07 | 298.56 | 582.00 |
| 0.50 | | 0.50 | | 267.38 | 222.18 | 290.00 |
| | | 0.75 | | 281.76 | 237.10 | 360.00 |
| | | 1.00 | | 290.51 | 260.07 | 445.00 |
| | | 1.25 | | 300.43 | 274.33 | 482.00 |
| 0.60 | | 0.50 | | 238.08 | 194.66 | 280.00 |
| | | 0.75 | | 252.22 | 209.35 | 355.00 |
| | | 1.00 | | 260.86 | 232.08 | 435.00 |
| | | 1.25 | | 270.59 | 246.15 | 465.00 |
| 0.00 | 0.75 | 0.50 | | 349.30 | 286.32 | 405.00 |
| | | 0.75 | | 372.90 | 310.68 | 455.00 |
| | | 1.00 | | 387.21 | 348.00 | 505.00 |
| | | 1.25 | | 403.94 | 371.81 | 535.00 |
| 0.30 | | 0.50 | | 372.26 | 307.97 | 475.00 |
| | | 0.75 | | 396.13 | 332.60 | 515.00 |
| | | 1.00 | | 410.57 | 370.19 | 545.00 |
| | | 1.25 | | 427.51 | 394.23 | 558.00 |
| 0.40 | | 0.50 | | 354.35 | 291.09 | 512.00 |
| | | 0.75 | | 378.02 | 315.51 | 558.00 |
| | | 1.00 | | 392.35 | 352.89 | 585.00 |
| | | 1.25 | | 409.12 | 376.74 | 605.00 |
| 0.50 | | 0.50 | | 329.08 | 267.25 | 380.00 |
| | | 0.75 | | 352.44 | 291.37 | 430.00 |
| | | 1.00 | | 366.62 | 328.44 | 478.00 |
| | | 1.25 | | 383.16 | 352.04 | 495.00 |
| 0.60 | | 0.50 | | 299.66 | 239.50 | 375.00 |
| | | 0.75 | | 322.67 | 263.29 | 422.00 |
| | | 1.00 | | 336.68 | 300.00 | 462.00 |
| | | 1.25 | | 352.94 | 323.31 | 482.00 |
| 0.00 | 1.00 | 0.50 | | 412.08 | 333.15 | 438.00 |
| | | 0.75 | | 445.94 | 367.96 | 470.00 |
| | | 1.00 | | 466.40 | 421.14 | 518.00 |
| | | 1.25 | | 490.88 | 455.78 | 545.00 |

**Table 4** continued

| ri/ro | h1/B | Fibre content (%) | RD (%) | UBC (kN/m²) | | |
|-------|------|-------------------|--------|-------------|--------------|--------------|
| | | | | Direct shear | Triaxial shear | Experimental |
| 0.30 | 0.50 | | | 435.12 | 354.97 | 501.00 |
| | 0.75 | | | 469.34 | 390.13 | 541.00 |
| | 1.00 | | | 489.99 | 443.69 | 562.00 |
| | 1.25 | | | 514.76 | 478.63 | 580.00 |
| 0.40 | 0.50 | | | 417.15 | 337.96 | 540.00 |
| | 0.75 | | | 451.09 | 372.84 | 575.00 |
| | 1.00 | | | 471.60 | 426.10 | 608.00 |
| | 1.25 | | | 496.14 | 460.81 | 645.00 |
| 0.50 | 0.50 | | | 391.77 | 313.92 | 428.00 |
| | 0.75 | | | 425.31 | 348.42 | 462.00 |
| | 1.00 | | | 445.62 | 401.27 | 505.00 |
| | 1.25 | | | 469.84 | 435.64 | 540.00 |
| 0.60 | 0.50 | | | 362.24 | 285.96 | 408.00 |
| | 0.75 | | | 395.32 | 320.00 | 442.00 |
| | 1.00 | | | 415.39 | 372.37 | 485.00 |
| | 1.25 | | | 439.25 | 406.34 | 498.00 |

test has been compared with the experimental UBC. Major findings of this study are as follows:

- Stress–strain response gets significantly influenced by the introduction of randomly distributed fibres in the sand. When fibre content is increased from 0.50 to 1.25%, the peak shear stress (70% RD; normal stress $= 200$ kN/m²) increases from 159.08 to 172.90 kN/m² and peak deviator stress (70% RD; confining pressure $= 200$ kN/m²) increases from 527.33 to 629.34 kN/m². Moreover, with the addition of fibres into sand, post peak reduction in terms of shear stress is deceased significantly; especially when fibre-reinforced sand is compacted at 70% RD.
- Relative density affects the peak shear stress of the unreinforced and fibre-reinforced sand. When the RD of unreinforced sand is increased from 50 to 70%, the peak shear stress (normal stress $= 200$ kN/m²) increases from 124.97 to 147.99 kN/m², and peak deviator stress (normal stress $= 200$ kN/m²) increases from 404.86 to 450.92 kN/m².
- Increasing the normal stress or confining pressure on same sand sample influences both the peak shear stress, and deviator stress. On increasing the normal stress, of unreinforced sand when compacted at 70% RD, from 50 to 200 kN/m², the peak shear stress increases from 37 to 147.99 kN/m², and peak deviator stress increases from 112.73 to 450.92 kN/m².

- An empirical equation has been proposed to find out UBC of ring footings. UBC calculated using shear strength parameters obtained from direct shear tests was found to be more than that of the UBC calculated by using shear strength parameters obtained from triaxial shear tests.
- Ultimate bearing capacity of ring footing with radius ratio of 0.4 was found to be more than that of circular footing for same testing conditions. UBC for circular footing (h1/B $= 1.0$; 1.25% Fibre in RDFS layer) is 545 kN/m² and for ring footing with radius ratio of 0.4, for same testing condition is observed as 645 kN/m².
- Increasing the percentage of fibres in RDFS increases the Ultimate bearing capacity and reduces the corresponding settlement. Optimum value of fibre percentage is observed as 1% for this study and increasing the percentage of fibres beyond this value, rate of increase in ultimate bearing capacity is reduced. BCR value for circular footing (h1/B $= 0.5$) at 0.5, 0.75, 1.0, and 1.25% is 1.93, 2.13, 2.45, and 2.63, respectively.
- Increasing the thickness of RDFS layer overlying unreinforced sand improves BCR values. BCR values for ring footing with radius ratio of 0.4 (0.5% fibre), for h1/B $= 0.5$, 0.75, and 1.0 are 2.15, 2.75, and 2.90, respectively.

**Table 5** Comparison of UBC calculated by using parameters of direct shear and triaxial shear tests with the experimental

| $r_i/r_o$ | $h1/B$ | Fibre content (%) | RD (%) | UBC (kN/m²) Direct shear | Triaxial shear | Experimental |
|---|---|---|---|---|---|---|
| 0.00 | 0.00 | 0.00 | 70.00 | 173.64 | 173.64 | 225.00 |
| 0.30 | | | | 197.23 | 197.23 | 262.00 |
| 0.40 | | | | 172.00 | 172.00 | 275.00 |
| 0.50 | | | | 147.02 | 147.02 | 179.00 |
| 0.60 | | | | 117.94 | 117.94 | 170.00 |
| 0.00 | 0.50 | 0.50 | | 330.86 | 294.87 | 400.00 |
| | | 0.75 | | 359.79 | 308.74 | 435.00 |
| | | 1.00 | | 383.39 | 328.21 | 500.00 |
| | | 1.25 | | 399.49 | 351.54 | 510.00 |
| 0.30 | | 0.50 | | 355.59 | 318.83 | 442.00 |
| | | 0.75 | | 384.69 | 332.84 | 506.00 |
| | | 1.00 | | 408.46 | 352.51 | 545.00 |
| | | 1.25 | | 424.65 | 376.19 | 565.00 |
| 0.40 | | 0.50 | | 329.14 | 293.20 | 459.00 |
| | | 0.75 | | 358.05 | 307.06 | 555.00 |
| | | 1.00 | | 381.65 | 326.52 | 585.00 |
| | | 1.25 | | 397.74 | 349.83 | 595.00 |
| 0.50 | | 0.50 | | 302.95 | 267.82 | 339.00 |
| | | 0.75 | | 331.67 | 281.53 | 420.00 |
| | | 1.00 | | 355.10 | 300.78 | 468.00 |
| | | 1.25 | | 371.09 | 323.72 | 500.00 |
| 0.60 | | 0.50 | | 272.47 | 238.28 | 340.00 |
| | | 0.75 | | 300.97 | 251.81 | 418.00 |
| | | 1.00 | | 324.20 | 270.83 | 465.00 |
| | | 1.25 | | 340.07 | 293.34 | 500.00 |
| 0.00 | 0.75 | 0.50 | | 419.86 | 358.44 | 458.00 |
| | | 0.75 | | 467.62 | 380.76 | 478.00 |
| | | 1.00 | | 508.41 | 412.34 | 530.00 |
| | | 1.25 | | 536.35 | 451.66 | 560.00 |
| 0.30 | | 0.50 | | 445.16 | 382.59 | 500.00 |
| | | 0.75 | | 493.18 | 405.12 | 540.00 |
| | | 1.00 | | 534.21 | 436.99 | 575.00 |
| | | 1.25 | | 562.30 | 476.84 | 600.00 |
| 0.40 | | 0.50 | | 418.10 | 356.76 | 542.00 |
| | | 0.75 | | 465.84 | 379.06 | 581.00 |
| | | 1.00 | | 506.61 | 410.62 | 630.00 |
| | | 1.25 | | 534.55 | 449.91 | 650.00 |
| 0.50 | | 0.50 | | 391.31 | 331.18 | 435.00 |
| | | 0.75 | | 438.76 | 353.25 | 471.00 |
| | | 1.00 | | 479.28 | 384.51 | 500.00 |
| | | 1.25 | | 507.06 | 423.24 | 538.00 |
| 0.60 | | 0.50 | | 360.13 | 301.42 | 402.00 |
| | | 0.75 | | 407.24 | 323.22 | 460.00 |
| | | 1.00 | | 447.48 | 354.12 | 500.00 |
| | | 1.25 | | 475.08 | 392.20 | 541.00 |
| 0.00 | 1.00 | 0.50 | | 518.97 | 423.98 | 460.00 |
| | | 0.75 | | 590.40 | 455.72 | 495.00 |
| | | 1.00 | | 652.73 | 500.95 | 555.00 |
| | | 1.25 | | 698.10 | 561.44 | 575.00 |

**Table 5** continued

| $r_i/r_o$ | $h1/B$ | Fibre content (%) | RD (%) | UBC (kN/m$^2$) | | |
|---|---|---|---|---|---|---|
| | | | | Direct shear | Triaxial shear | Experimental |
| 0.30 | 0.50 | | | 544.83 | 448.31 | 532.00 |
| | 0.75 | | | 616.62 | 480.34 | 575.00 |
| | 1.00 | | | 679.27 | 525.96 | 600.00 |
| | 1.25 | | | 724.84 | 587.15 | 610.00 |
| 0.40 | 0.50 | | | 517.17 | 422.28 | 580.00 |
| | 0.75 | | | 588.57 | 454.00 | 615.00 |
| | 1.00 | | | 650.88 | 499.21 | 655.00 |
| | 1.25 | | | 696.24 | 559.65 | 670.00 |
| 0.50 | 0.50 | | | 489.77 | 396.51 | 462.00 |
| | 0.75 | | | 560.80 | 427.92 | 500.00 |
| | 1.00 | | | 622.77 | 472.72 | 540.00 |
| | 1.25 | | | 667.93 | 532.42 | 580.00 |
| 0.60 | 0.50 | | | 457.89 | 366.51 | 440.00 |
| | 0.75 | | | 528.47 | 397.58 | 460.00 |
| | 1.00 | | | 590.06 | 441.89 | 505.00 |
| | 1.25 | | | 634.98 | 500.73 | 542.00 |

# References

1. Egorov KE (1965) Calculation of bed for foundation with ring footing, In: Sixth Int. Conf. Soil Mech. Found. Eng.: pp. 41–45.
2. Egorov KE, Konovalov PA, Kitaykina OV, Salnikov LF, Zinovyev AV (1977) Soil deformation under circular footing. In: 9th Int Conf SMFE, Tokyo, pp 489–492
3. Saha MC (1978) Ultimate bearing capacity of ring footings on sand, ME dissertation, University of Roorkee, Roorkee, India
4. Haroon M, Misra SK (1980) A study on the behaviour of annular footings on sand. In: Indian Geotech Soc IGC-80, Bombay, pp 87–91
5. Kakroo AK (1985) Bearing capacity of rigid annular foundations under vertical loads, PhD dissertation, University of Roorkee, Roorkee, India, 1985
6. Al-Sanad HA, Ismael NF, Brenner RP (1993) Settlement of circular and ring plates in very dense calcareous sands. J Geotech Eng 119(4):622–638
7. Ismael NF (1996) Loading tests on circular and ring plates in very dense cemented sands. J Geotech Eng 122(4):281–287
8. Boushehrian JH, Hataf N (2003) Experimental and numerical investigation of the bearing capacity of model circular and ring footings on reinforced sand. J Geotext Geomembr 21(4):241–256
9. Kumar J, Ghosh P (2005) Bearing capacity factor $N_\gamma$ for ring footings using the method of characteristics. Can Geotech J 42(5):1474–1484
10. Karaulov AM (2005) Static solution of the limiting-pressure problem for ring foundations on soil beds. Soil Mech Found Eng 42(6):189–194
11. Karaulov AM (2006) Experimental and theoretical research on the bearing capacity of Ring-Foundation beds. Soil Mech Found Eng 43(2):37–40
12. Laman M, Yildiz A (2007) Numerical studies of ring foundations on geogrid- reinforced sand. Geosynth. Int. 14 (2):52–64
13. Zhao L, Wang JH (2008) Vertical bearing capacity for ring footings. Comput Geotech 35(2):292–304
14. Benmebarek S, Remadna MS, Benmebarek N, Belounar L (2012) Numerical evaluation of the bearing capacity factor Ny' of ring footings. Comput Geotech 44:132–138
15. Naderi E, Hataf N (2014), Model testing and numerical investigation of interference effect of closely spaced ring and circular footings on reinforced sand. Geotext Geomembr 42(3):191–200
16. Kumar J, Chakraborty M (2015) Bearing capacity factors for ring foundations. J Geotech Geoenviron Eng 141(10):1–7
17. Lee JK, Jeong S, Lee S (2016) Undrained bearing capacity factors for ring footings in heterogeneous soil. Comput Geotech 75:103–111
18. Naseri M, Hosseininia ES (2015) Elastic settlement of ring foundations. Soils Found 55(2):284–295
19. Gray DH, Ohashi H (1983) Mechanics of fiber reinforcement in sand. J Geotech Eng 109(3):335–353
20. Gray DH, Al-Refeai T (1986) Behavior of fabric- versus fiber-reinforced sand. J Geotech Eng 112(8):804–820
21. Freitag DR (1986) Soil randomly reinforced with fibers. J Geotech Eng 112(8):823–826
22. Michalowski RL, Zhao A (1996) Failure of fiber-reinforced granular soils. J. Geotech. Eng. 122(3):226–234
23. Michalowski RL, Čermák J (2003) Triaxial compression of sand reinforced with fibers. J Geotech Geoenviron Eng 129(2):125–136
24. Consoli NC, Casagrande MDT, Prietto PDM, Thomé A (2003) Plate load test on fiber-reinforced soil. J Geotech Geoenviron Eng 129(10):951–955
25. Consoli NC, Vendruscolo AM, Prietto PDM (2003) Behavior of plate load tests on soil layers improved with cement and fiber. J Geotech Geoenviron Eng 129(1):96–101
26. Sivakumar Babu GL, Vasudevan AK (2008) Strength and stiffness response of coir fiber-reinforced tropical soil. J Mater Civ Eng 20(9):571–577
27. Yetimoglu T, Inanir M, Inanir OE (2005) A study on bearing capacity of randomly distributed fiber-reinforced sand fills overlying soft clay. Geotext Geomembr 23(2):174–183
28. Diambra A, Ibraim E, Wood DM Russell AR, (2010) Geotextiles and geomembranes fibre reinforced sands†‾: experiments and modelling. Geotext Geomembr 28(3):238–250
29. Sadek S, Najjar SS, Freiha F (2010) Shear strength of fiber-reinforced sands. J Geotech Geoenviron Eng 136(3):490–499

30. Li C, Zornberg JG (2013) Mobilization of reinforcement forces in fiber reinforced soil, J Geotech Geoenviron Eng 139(1):107–115
31. Kumar A, Gupta D (2016) Behavior of cement-stabilized fiber-reinforced pond ash, rice husk ash-soil mixtures. Geotext Geomembr 44(3):466–474
32. ASTM D3080// D3080M-11 (2011) Standard Test Method for Direct Shear Test of Soils Under Consolidated Drained Conditions, ASTM Int. West Conshohocken
33. ASTM D7181-11 (2011) Method for Consolidated Drained Triaxial Compression Test for Soils, ASTM Int. West Conshohocken
34. Terzaghi K (1943) Theoretical soil mechanics. John Wiley & Sons, New York
35. Sharma V (2017) Circular and ring footings resting on randomly distributed fiber reinforced sand, PhD dissertation (under preparation), Dr. B R Ambedkar National Institute of Technology, Jalandhar, Punjab, India
36. Shukla SK (2016) An introduction to geosynthetic engineering. CRC press, Taylor & Francis, London (**Ebook**)
37. Sawwaf MEl, Nazir A (2012) Behavior of eccentrically loaded small-scale ring footings resting on reinforced layered soil, J Geotech Geoenviron Eng 138(3):376–384